

Enhanced Mechanical Stability of Microtubules Polymerized with a Slowly Hydrolyzable Nucleotide Analogue

Kathleen M. Munson,[†] Philipose G. Mulugeta, and Zachary J. Donhauser*

Department of Chemistry, Vassar College, Poughkeepsie, New York 12604

Received: February 28, 2007; In Final Form: April 4, 2007

Atomic force microscopy (AFM) has been used to investigate the local mechanical and structural properties of microtubules polymerized using guanylyl- α - β -methylene diphosphonate (GMPCPP), a slowly hydrolyzable analogue of guanosine triphosphate. Using a combination of AFM imaging and local force spectroscopy, GMPCPP-polymerized microtubules have been qualitatively and quantitatively compared to paclitaxel-stabilized microtubules. GMPCPP-polymerized microtubules qualitatively display a greater resistance to destruction by the AFM probe tip during imaging and during deformation measurements and maintain structural details after indentation. In addition, using force spectroscopy taken during the indentation and collapse of individual microtubules with the AFM probe tip, an effective spring constant of the microtubule wall (k_{MT}) for both types of microtubules was determined. The average k_{MT} of GMPCPP-polymerized microtubules, 0.172 N/m, is more than twice that of paclitaxel-stabilized microtubules. These results complement previously reported measurements of bending experiments on GMPCPP-polymerized and paclitaxel-stabilized microtubules.

Introduction

Microtubules are one of the three primary components of the cytoskeleton found in eukaryotic cells.¹ They provide mechanical stability and structural support for the maintenance of cell shape, support intracellular transport, and can act as small molecular machines that perform dynamic processes within cells when they undergo cycles of polymerization and depolymerization, as in mitosis. Hence, studying the structural and mechanical properties of microtubules, especially the regulation of polymerization and depolymerization, can provide a more complete understanding of their physiological roles.

Free tubulin exists as dimers that associate head-to-tail to form protofilaments. Between 8 and 17 protofilaments bind laterally to create the cylindrical microtubule structure.² Microtubules have been observed to undergo periods of growth and rapid depolymerization, creating what is referred to as “dynamic instability,” a process that is closely linked to the hydrolysis of guanosine triphosphate (GTP) bound between tubulin dimers in the microtubule lattice.³ Microtubules containing hydrolyzed GTP are intrinsically unstable, hindering direct *in vitro* studies of their mechanical properties. Therefore, the slowly hydrolyzable GTP analogue guanylyl- α - β -methylene-diphosphonate (GMPCPP) has been used to mimic GTP-containing protofilaments for *in vitro* studies of microtubule structure due to the similar structures and tubulin-binding affinities of GTP and GMPCPP.^{4–9} Cryoelectron microscopy studies have shown that the intrinsic curvature between tubulin subunits within protofilaments is greater in guanosine diphosphate (GDP)-containing protofilaments than in GMPCPP-containing protofilaments.⁵ However, if protofilaments are

constrained to a straight orientation within the microtubule lattice, the energy released during hydrolysis of GTP results in accumulation of strain in the microtubule. Thus, GTP hydrolysis prepares the microtubule for rapid depolymerization to release the increased strain within the lattice. The most popular models of the GTP hydrolysis cycle in microtubules require the existence of a GTP cap that prevents microtubule depolymerization. In these models, the endmost tubulin dimers in the microtubule contain GTP, maintain a straight protofilament structure and a cylindrical microtubule, and prevent rapid depolymerization.^{3,6} However, direct observation of the GTP cap has proven difficult and has prevented a more precise understanding of the relationship between GTP hydrolysis, microtubule mechanics, and dynamic instability.

Previous measurements and subsequent models of the mechanical properties of microtubules have focused most heavily on bending experiments in which bending of stabilized microtubules is induced by thermal fluctuations or optical trapping and is observed and quantified by optical microscopy. Paclitaxel, microtubule-associated proteins (MAPs), and GMPCPP have been used to stabilize microtubules in these experiments. Most of these studies consider the microtubule as a uniform hollow cylinder.^{4,10–17} However, recent studies of paclitaxel-stabilized microtubules by intentional deformation of the microtubule cylinder using AFM have begun to probe mechanical properties of microtubules on a local level and have used models of the microtubule as a cylindrical shell with realistic molecular-level structure.^{18–21} Although paclitaxel stabilizes microtubules from depolymerization and allows for *in vitro* studies of microtubule mechanical and structural properties, the structural rigidity of paclitaxel-stabilized microtubules has been found to vary significantly in GDP-containing, GMPCPP-containing, and MAP-stabilized microtubules in bending experiments,⁴ limiting the applicability of paclitaxel in studies of microtubule me-

* Corresponding author. E-mail: zadonhauser@vassar.edu.

[†] Present address: Developmental Biology Laboratory, Cardiovascular Research Center, Massachusetts General Hospital, Charlestown, MA 02129.

chanical stability. In this study, the local mechanical and structural properties of GMPCPP-polymerized microtubules were probed using AFM in order to better understand the stabilizing effects of unhydrolyzed GTP and to relate this to models of the GTP cap.

Experimental Methods

Tubulin was purified from fresh calf brain according to established protocols.²² For complementary optical microscopy, some cycled tubulin was labeled with carboxytetramethylrhodamine (Invitrogen, Carlsbad, CA).²³ Paclitaxel-stabilized microtubules were polymerized at 37 °C in BRB80 buffer (80 mM K-pipes, 1 mM EGTA, 1 mM MgCl₂, pH 6.85) containing 4 mM MgCl₂, 1 mM GTP, 5% DMSO, and 32 μM cycled tubulin for 20 min and diluted 100-fold into room temperature BRB80 containing 100 μM paclitaxel (Sigma-Aldrich, St. Louis, MO). GMPCPP was synthesized according to established protocols.^{7,8} GMPCPP-polymerized microtubules were polymerized at 37 °C in BRB80 containing 4 mM MgCl₂, 1 mM GMPCPP, 5% DMSO, and 0.25 μM cycled tubulin for 4–6 h.⁷ The incubating solution was replenished with 0.2 μM cycled tubulin every 30 min to sustain microtubule polymerization.⁷ GMPCPP-polymerized microtubules were diluted 100-fold into BRB80 before imaging. Force data were collected over a period of several days, during which microtubule solutions were prepared immediately prior to AFM imaging.

To prepare AFM substrates, freshly cleaved mica sheets (Ted Pella, Redding, CA) were exposed to aminopropyltriethoxysilane (APTES) in a desiccator.²⁴ AFM imaging and force curve collection were performed using a Veeco Multimode/Nanoscope IIIa operating in TappingMode (Veeco Metrology, Inc., Santa Barbara, CA). Imaging of microtubules and collection of force data were performed under buffer at room temperature using oxide-sharpened triangular Si₃N₄ cantilevers with nominal spring constants of 0.06 N/m and a nominal tip radius of curvature of 10 nm (Veeco Metrology, Inc., Santa Barbara, CA). The cantilevers were calibrated using the reference cantilever method²⁵ and found to have spring constants of ~0.1 N/m. Multiple cantilevers were used in order to account for variability among cantilevers. Microtubules were immobilized on APTES-mica by exposing the surface to the microtubule solution, and AFM imaging was performed immediately under the same solution. Force measurements were obtained without Tapping-Mode cantilever oscillation, and after the collection of a force curve, the microtubule was reimaged in TappingMode to examine the region of indentation. Calibration curves of cantilever sensitivity were obtained over regions of the mica surface that did not contain adsorbed protein.

The force curves were analyzed using MATLAB (The MathWorks, Natick, MA). Curves of cantilever deflection versus distance were converted into force versus indentation by comparing microtubule curves to cantilever sensitivity curves and by using the calibrated spring constant values of the cantilevers used for microtubule indentation. In accordance with previous AFM indentation experiments, analysis was focused on the linear regime of the microtubule indentation, which occurs with indentation up to ~4 nm. The slope of the curve in this region reveals k_{MT} , which could then be used to estimate the Young's modulus of the microtubules using a previously reported thin-shell, finite-element model of the microtubule.^{19,21}

Results and Discussion

Figure 1 shows AFM images comparing GMPCPP-polymerized microtubules (Figure 1B) and paclitaxel-stabilized mi-

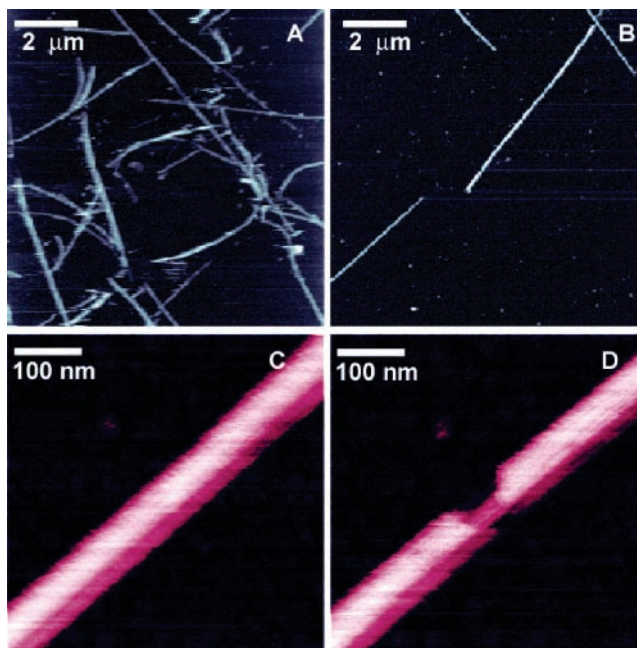


Figure 1. AFM images of (A) paclitaxel-stabilized and (B) GMPCPP-polymerized microtubules imaged under buffer. GMPCPP-polymerized microtubules are straighter and less numerous than paclitaxel-stabilized microtubules in similar scan sizes. (C) A higher-resolution image of a GMPCPP-polymerized microtubule. (D) The same region of the microtubule after a local applied force of ~1.7 nN. The linear structure of the protofilaments (running along the microtubule axis) is visible in the damaged region after the upper layer of tubulin was removed by the AFM probe tip.

crotofilaments (Figure 1A) immobilized on APTES-mica. The surface coverage of GMPCPP-polymerized microtubules was lower than paclitaxel-stabilized microtubules, likely due to the lower concentration of the GMPCPP-polymerized microtubules in solution. GMPCPP-polymerized microtubules are generally more uniform in diameter and length and appear straighter than paclitaxel-stabilized microtubules. Under local application of high force (>1.5 nN) with the AFM tip, the upper layer of tubulin can be removed. This force is greater than that which has been reported for paclitaxel microtubules.²⁶ Although it is difficult to resolve the microtubule substructure (protofilaments) on the outer surface of the GMPCPP-polymerized microtubules (Figure 1C), the removal of the upper tubulin layer reveals microtubule substructure inside the microtubule (Figure 1D). Protofilaments are visible as linear striations in the damaged area of the microtubule. Although the outer surface of the microtubule has deeper grooves between protofilaments,²⁷ the protofilament structure might be more easily imaged on the flatter inner surface because objects with high aspect ratios (e.g., the microtubule) are more susceptible to imaging convolutions.

Microtubules are known to polymerize *in vitro* with varying numbers of protofilaments under various buffer conditions.² Cryoelectron microscopy studies have revealed that GMPCPP-polymerized microtubules most often contain 14 protofilaments rather than the 13 protofilaments most often found in paclitaxel-stabilized microtubules.⁷ The diameters of the GMPCPP-polymerized microtubules imaged typically ranged from 30 to 40 nm, whereas those of paclitaxel-stabilized microtubules typically ranged from 25 to 30 nm. AFM tip broadening can distort the apparent lateral dimensions of objects with high aspect ratios (such as microtubules) (Figure 2A, D); therefore the diameters of microtubules were estimated from the heights as measured by AFM (Figure 2C, F). Two factors may contribute to the increased height of GMPCPP-polymerized

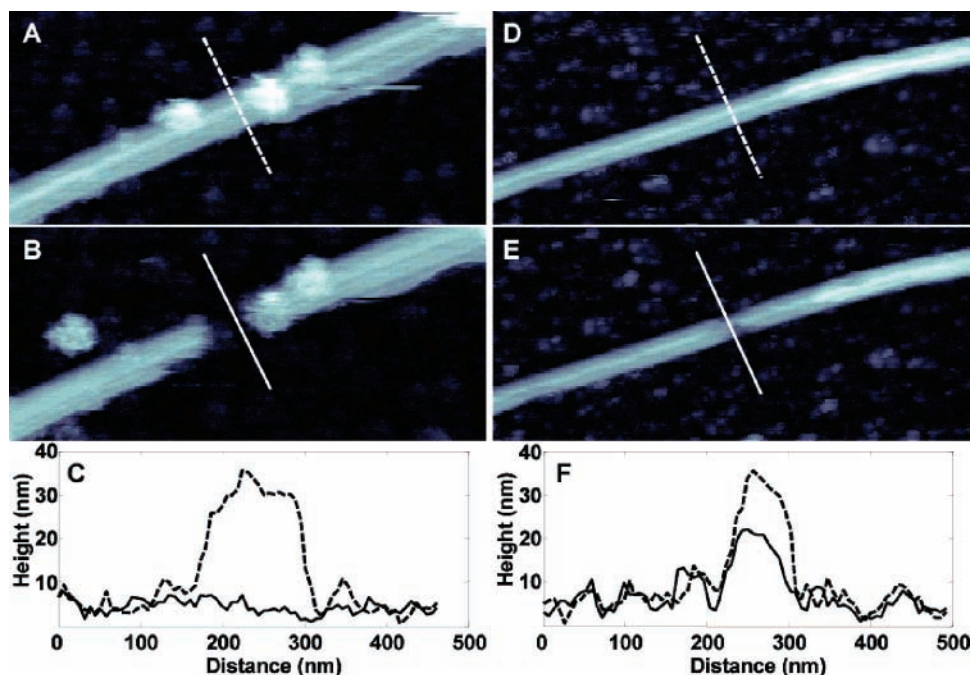


Figure 2. (A, B) A comparison of height data collected over paclitaxel-stabilized microtubules before (A) and after (B) the collection of force data. (C) Cross sections reveal that the cylindrical structure of paclitaxel-stabilized microtubules is destroyed entirely under an applied force of ~ 0.8 nN by the AFM probe tip. (D, E) A comparison of height data collected over GMPCPP-polymerized microtubules before (D) and after (E) the collection of force data. (F) Cross sections show that the cylindrical structure of GMPCPP-polymerized microtubules remains intact after an applied force of ~ 0.9 nN. In C and F, height profiles across the microtubules correspond to the lines indicated in A–B and D–E, respectively.

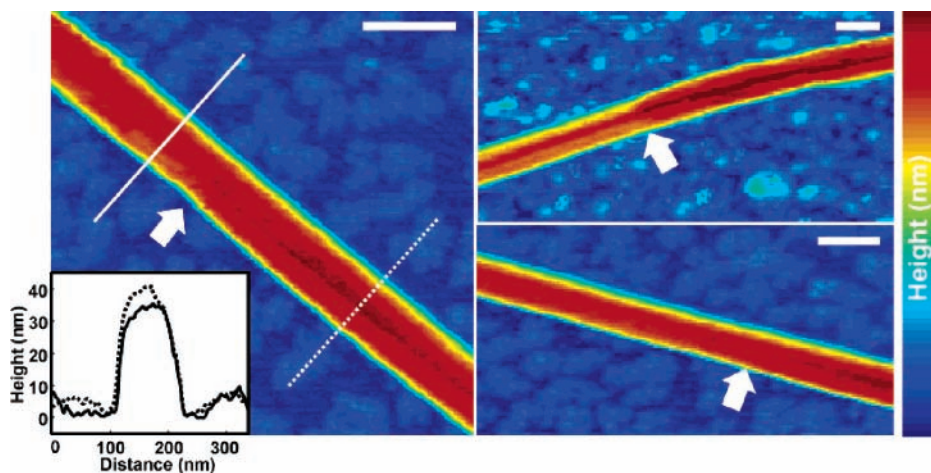


Figure 3. AFM height data collected over individual GMPCPP-polymerized microtubules reveals changes in microtubule diameters along their lengths. Abrupt changes in microtubule diameter (indicated by white arrows) from ~ 35 to ~ 40 nm (left, inset) may correspond to the changes in the number of protofilaments within the microtubule cylinder. The full vertical scale for the images is 42 nm. Scale bars: 100 nm.

microtubules: (1) the presence of a greater number of protofilaments in GMPCPP-polymerized microtubules or (2) AFM imaging artifacts due to their greater resistance to compression by the AFM probe tip, which might artificially enhance diameter differences between the two types of microtubules under comparable imaging conditions.

In addition to increased diameters, abrupt diameter changes were observed along the length of several GMPCPP-polymerized microtubules in AFM images (Figure 3). Height data from cross sections on either side of these diameter changes reveal differences in diameter of ~ 5 nm (Figure 3, inset). These changes in microtubule diameter may correspond to changes in the number of protofilaments within the microtubule lattice that have been reported previously.^{2,28,29} Interestingly, in previous AFM studies as well as in the current study, diameter changes have not been observed in paclitaxel-stabilized micro-

tubules.¹⁹ This observation has been explained using the argument that only the most stable (13-protofilament) paclitaxel-stabilized microtubules are able to withstand imaging with AFM.²¹ Since at least two different types (diameters) of GMPCPP-polymerized microtubules were observed, this is an indirect indication that GMPCPP has a greater stabilizing effect than paclitaxel. It is known that microtubules with a lattice different from an “ideal” 3-start, 13-protofilament lattice must accommodate some excess mechanical stress that arises from deviations in interprotofilament interactions from the “ideal” case.^{30,31} This excess mechanical stress results in a less stable microtubule. In contrast to paclitaxel, the stabilizing effect of GMPCPP is sufficient to allow AFM imaging of a different microtubule structure that deviates from the ideal case and is less favorable. Although specific microtubule geometries cannot be assigned from the data, higher-resolution AFM imaging may

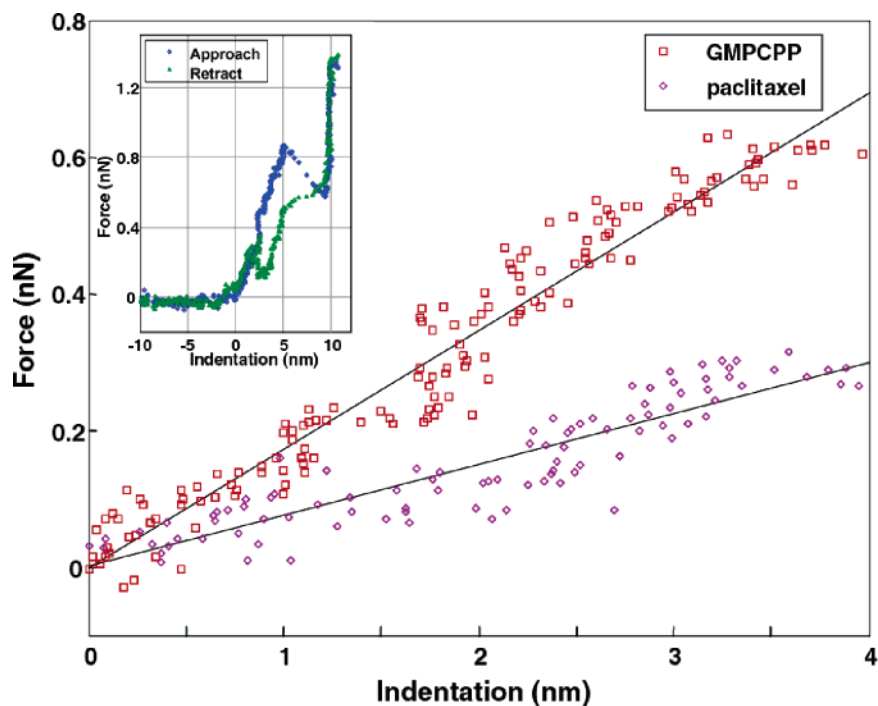


Figure 4. Representative force versus microtubule indentation data for paclitaxel-stabilized (diamonds) and GMPCPP-polymerized (squares) microtubules up to 4 nm of indentation. Within this portion of the force-versus-microtubule indentation data curve, the k_{MT} of GMPCPP-polymerized microtubules, as measured from the slope of the curve, is more than twice as great as the k_{MT} of paclitaxel-stabilized microtubules. (Inset) Individual force-versus-microtubule indentation curves collected over GMPCPP-polymerized microtubules show large discontinuities in both the approach and the retraction data. These discontinuities in the approach data indicate either the collapse of the microtubule cylinder or the severing of interprotofilament bonds. Discontinuities in the retraction curve may indicate restoration of the microtubule cylinder.

reveal the protofilament number, helicity of the lattice along the length of a GMPCPP-polymerized microtubule, or both.

It was also observed that GMPCPP-polymerized microtubules are more resistant to catastrophic deformation caused by the AFM probe tip than are paclitaxel-stabilized microtubules. This is demonstrated in Figure 2. The collection of a single force-versus-distance curve under high forces (~ 1 nN) on paclitaxel-stabilized microtubules causes the collapse and destruction of that region of the microtubule (Figure 2B). Height data taken over the indentation region after the collection of a force-versus-distance curve shows that all remnants of the microtubule have been removed (Figure 2C). In contrast, GMPCPP-polymerized microtubules resist catastrophic deformation after the application of a similar amount of force by the AFM probe tip (Figure 2E). The diameter of the indented microtubule is ~ 20 nm, indicating some damage to or deformation of the microtubule; however, this measured height is still greater than the thickness of a collapsed microtubule (Figure 2F). Therefore, despite significant indentation by the AFM probe tip, the structure of a GMPCPP-polymerized microtubule is largely maintained.

To obtain quantitative estimates of the stability of GMPCPP-polymerized microtubules compared to paclitaxel-stabilized microtubules, the force required to indent immobilized microtubules was measured. For both types of microtubules, application of low forces (< 300 – 400 pN) resulted in an approximately linear elastic response from the microtubule and little visible damage to the microtubule structure. Figure 4 shows representative force-versus-indentation curves that compare a GMPCPP-polymerized microtubule with a paclitaxel-stabilized microtubule. The data collected on the GMPCPP-polymerized microtubule reveals its increased structural rigidity. From the elastic region of 19 force-versus-distance curves collected over 5 GMPCPP-polymerized microtubules using several AFM tips, an average k_{MT} of 0.17 ± 0.05 N/m was found using the

calibrated cantilever spring constant of 0.1 N/m. This value is more than twice the k_{MT} of paclitaxel-stabilized microtubules, which was found to be 0.07 ± 0.03 N/m. The paclitaxel-stabilized microtubule value is in very good agreement with previously published AFM data.²¹ For both types of microtubules, measurements were made using several different tips, over several (at least 3) days, each time with fresh microtubule samples. Some of the variability in the values of k_{MT} likely arise from differences in experimental geometry (such as tip condition or microtubule adsorption geometry); however, previous experimental and theoretical studies have shown that variations in cantilever stiffness and tip radius have little effect on the average measured values of k_{MT} .²¹ Using a finite element model developed from previous indentation studies of paclitaxel-stabilized microtubules,^{19,21} it is possible to estimate the Young's modulus of the material for the two types of microtubules: for GMPCPP, 1.4 GPa,³² and for paclitaxel, 0.6 GPa. On the basis of bending experiments of GMPCPP-polymerized microtubules, a significant increase in the stiffness for GMPCPP-polymerized microtubules as compared to paclitaxel-stabilized microtubules is expected.⁴ However, it is important to note that local indentation measurements are probably more sensitive to the strength of the lateral interprotofilament bonds rather than the flexibility of protofilament bending, which is measured in bending experiments.¹⁹

Careful analysis of the retraction data of force-versus-indentation curves collected on GMPCPP-polymerized microtubules reveals discontinuities that represent the restoration of microtubule structure after the microtubule has undergone a collapse of ~ 5 nm (Figure 4, inset). Thus, discontinuities that appear in the approach data of force versus indentation curves of GMPCPP-polymerized microtubule are not catastrophically damaging to the microtubule and may represent either the collapse of the microtubule cylinder while the tubulin layers

remain intact or the separation of protofilaments that quickly reassemble as the AFM probe tip is withdrawn. Similar self-healing has been reported for paclitaxel-stabilized microtubules, but at much lower forces and only for 1 nm discontinuities.²¹ Although discontinuities were observed in force-versus-indentation curves (Figure 4, inset), to a large degree, GMPCPP-polymerized microtubules appeared structurally intact during reimaging.

The enhanced resistance to radial deformation that was observed for GMPCPP-polymerized microtubules has important implications for the GTP cap that is found in microtubules in vivo. The stabilizing effect of the GTP cap is thought to arise from its ability to restrict the outward curvature of individual protofilaments within the microtubule lattice and, thus, maintain the cylindrical shape of the microtubule. In contrast, the binding of paclitaxel is thought to relieve lattice strain by increasing the flexibility of the microtubule.⁹ Due to the differences in the stabilizing effects of the GTP cap and paclitaxel, the significant increase that was observed in the k_{MT} of GMPCPP-polymerized microtubules compared to paclitaxel-stabilized microtubules likely arises from stronger lateral interactions between protofilaments. These stronger lateral interactions would be ideal to resist the outward strain introduced by the intrinsic curvature of GDP protofilaments. These data suggest that a significant part of the stabilizing effect of the GTP cap in native microtubules is due to increased lateral bonds between protofilaments.

Conclusions

Using a combination of AFM imaging and force spectroscopy, it was demonstrated that microtubules polymerized with GMPCPP are more robust and resistant to radial compression than those stabilized by paclitaxel. By comparing the local structural properties of GMPCPP-polymerized microtubules and paclitaxel-stabilized microtubules, the stabilizing effect of GMPCPP can be better understood and applied to an understanding of a native microtubule's GTP cap on the basis of the structural differences between the two types of microtubules. Further studies that address GMPCPP-polymerized microtubules at different points along their length may help refine the current model and help elucidate anisotropic properties of the microtubule.³³ These local studies of GMPCPP-polymerized microtubules and their implications for existing models of microtubule mechanics can contribute to a better understanding of microtubules as dynamic elements of cells.

Acknowledgment. We thank W. Hancock and D. Jemiole for assistance with tubulin purification and E. Eberhardt and P. Lewis for assistance with this manuscript. Mr. Bob Franklin kindly provided calf brain. Continuing support from The Camille and Henry Dreyfus Foundation New Faculty Award Program and the Research Corporation Cottrell College Science Award are most gratefully acknowledged.

Supporting Information Available: Enlarged image of Figure 1C, D. This material is available free of charge via the Internet at <http://pubs.acs.org>.

References and Notes

- Alberts, B.; Johnson, A.; Lewis, J.; Raff, M.; Roberts, K.; Walter, P. *Molecular Biology of the Cell*, 4th ed.; Garland Science: New York, 2002.
- Chrétien, D.; Metoz, F.; Verde, F.; Karsenti, E.; Wade, R. H. *J. Cell Biol.* **1992**, *117*, 1031–1040.
- Mitchison, T.; Kirschner, K. *Nature* **1984**, *312*, 232–237.
- Mickey, B.; Howard, J. *J. Cell Biol.* **1995**, *130*, 909–917.
- Wang, H.-W.; Nogales, E. *Nature* **2005**, *435*, 911–915.
- Caplow, M.; Shanks, J. *Mol. Biol. Cell* **1996**, *7*, 663–675.
- Hyman, A. A.; Chrétien, D.; Arnal, I.; Wade, R. H. *J. Cell. Biol.* **1995**, *128*, 117–125.
- Vulevic, B.; Correia, J. J. *Biophys. J.* **1997**, *72*, 1357–1375.
- VanBuren, V.; Cassimeris, L.; Odde, D. J. *Biophys. J.* **2005**, *89*, 2911–2926.
- Cassimeris, L.; Gard, D.; Tran, P. T.; Erickson, H. P. *J. Cell Sci.* **2001**, *114*, 3025–3033.
- Felgner, H.; Frank, R.; Schliwa, M. *J. Cell Sci.* **1996**, *109*, 509–516.
- Venier, P.; Maggs, A. C.; Carlier, M. F.; Pantaloni, D. *J. Biol. Chem.* **1994**, *269*, 13353–13360.
- Gittes, F.; Mickey, B.; Nettleton, J.; Howard, J. *J. Cell Biol.* **1993**, *120*, 923–934.
- Kurz, J. C.; Williams, R. C., Jr. *Biochemistry* **1995**, *34*, 13374–13380.
- Janson, M. E.; Dogterom, M. *Biophys. J.* **2004**, *87*, 2723–2736.
- Kikumoto, M.; Kurachi, M.; Tosa, V.; Tashiro, H. *Biophys. J.* **2006**, *90*, 1687–1696.
- Vinckier, A.; Dumortier, C.; Engelborghs, Y.; Hellemans, L. *J. Vac. Sci. Technol., B* **1996**, *14*, 1427–1431.
- Kis, A.; Kasas, S.; Babić, B.; Kulik, A. J.; Benoît, W.; Briggs, G. A. D.; Schönberger, C.; Catsicas, S.; Forró, L. *Phys. Rev. Lett.* **2002**, *89*, 2481011–2481014.
- de Pablo, P. J.; Schaap, I. A. T.; MacKintosh, F. C.; Schmidt, C. F. *Phys. Rev. Lett.* **2003**, *91*, 981011–981014.
- Kasas, S.; Kis, A.; Riederer, B. M.; Forró, L.; Dietler, G.; Catsicas, S. *Chem. Phys. Chem.* **2004**, *5*, 252–257.
- Schaap, I. A. T.; Carrasco, C.; de Pablo, P. J.; MacKintosh, F. C.; Schmidt, C. F. *Biophys. J.* **2006**, *91*, 1521–1531.
- Lee, Y. C.; Samson, F. E.; Houston, L. L.; Himes, R. H. *J. Neurobiol.* **1974**, *5*, 317–330.
- This protocol can be found at the following URL: <http://mitchison.med.harvard.edu/protocols>.
- Lyubchenko, Y.; Shlyakhtenko, L.; Harrington, R.; Oden, P.; Lindsay, S. *Proc. Natl. Acad. Sci. U.S.A.* **1993**, *90*, 2137–2140.
- Tortonese, M.; Kirk, M. *Proc. SPIE* **1997**, *3009*, 53–60.
- Schaap, I. A. T.; de Pablo, P. J.; Schmidt, C. F. *Eur. Biophys. J.* **2004**, *33*, 462–467.
- Nogales, E.; Wolf, S. G.; Downing, K. H. *Nature* **1998**, *391*, 199–203.
- Pierson, G. B.; Burton, D. J.; Himes, T. H. *J. Cell Biol.* **1978**, *76*, 223–228.
- Arnal, I.; Wade, R. H. *Curr. Biol.* **1995**, *5*, 900–908.
- Chrétien, D.; Fuller, S. D. *J. Mol. Biol.* **2000**, *298*, 663–676.
- Hunyadi, V.; Chrétien, D.; Jánosi, I. M. *J. Mol. Biol.* **2005**, *348*, 927–938.
- Note that this value is calculated for the geometry of a 3-start, 13-protofilament microtubule. On the basis of these data and the observations of others, GMPCPP-polymerized microtubules probably do not have this geometry. Therefore, this value is presented only as an estimate of the Young's modulus.
- Pampaloni, F.; Lattanzi, G.; Jonas, A.; Surrey, T.; Frey, E.; Florin, E. L. *Proc. Nat. Acad. Sci.* **2006**, *103*, 10248–10253.